Engineering *Kluyveromyces marxianus* as a Robust Synthetic Biology Platform Host

Paul Cernak,[a] Raissa Estrela,[a] Snigdha Poddar,[a,b] Jeffrey M. Skerker,[c,d] Ya-Fang Cheng,[e] Annika K. Carlson,[c] Berling Chen,[f] Victoria M. Glynn,[g] Monique Furlan,[h] Owen W. Ryan,[a] Marie K. Donnelly,[i] Adam P. Arkin,[c,d,j] John W. Taylor,[i] Jamie H. D. Cate[a,f,k]

[a]Department of Molecular and Cell Biology, University of California, Berkeley, California, USA

[b]Innovative Genomics Institute, University of California, Berkeley, California, USA

[c]Department of Bioengineering, University of California, Berkeley, California, USA

[d]Biological Systems and Engineering Division, Lawrence Berkeley National Laboratory, Berkeley, California, USA

[e]Energy Biosciences Institute, Berkeley, California, USA

[f]Department of Chemistry, University of California, Berkeley, California, USA

[g]Department of Environmental Science, Policy, and Management, University of California, Berkeley, California, USA

[h]Department of Genetics, Evolution and Bioagents, University of Campinas, Campinas, São Paulo, Brazil

[i]Department of Plant and Microbial Biology, University of California, Berkeley, California, USA

[j]Environmental Genomics and Systems Biology Division, Lawrence Berkeley National Laboratory, Berkeley, California, USA

[k]Molecular Biophysics and Integrated Bioimaging, Lawrence Berkeley National Laboratory, Berkeley, California, USA

ABSTRACT Throughout history, the yeast *Saccharomyces cerevisiae* has played a central role in human society due to its use in food production and more recently as a major industrial and model microorganism, because of the many genetic and genomic tools available to probe its biology. However, *S. cerevisiae* has proven difficult to engineer to expand the carbon sources it can utilize, the products it can make, and the harsh conditions it can tolerate in industrial applications. Other yeasts that could solve many of these problems remain difficult to manipulate genetically. Here, we engineered the thermotolerant yeast *Kluyveromyces marxianus* to create a new synthetic biology platform. Using CRISPR-Cas9 (clustered regularly interspaced short palindromic repeats with Cas9)-mediated genome editing, we show that wild isolates of *K. marxianus* can be made heterothallic for sexual crossing. By breeding two of these mating-type engineered *K. marxianus* strains, we combined three complex traits—thermotolerance, lipid production, and facile transformation with exogenous DNA—into a single host. The ability to cross *K. marxianus* strains with relative ease, together with CRISPR-Cas9 genome editing, should enable engineering of *K. marxianus* isolates with promising lipid production at temperatures far exceeding those of other fungi under development for industrial applications. These results establish *K. marxianus* as a synthetic biology platform comparable to *S. cerevisiae*, with naturally more robust traits that hold potential for the industrial production of renewable chemicals.

IMPORTANCE The yeast *Kluyveromyces marxianus* grows at high temperatures and on a wide range of carbon sources, making it a promising host for industrial biotechnology to produce renewable chemicals from plant biomass feedstocks. However, major genetic engineering limitations have kept this yeast from replacing the commonly used yeast *Saccharomyces cerevisiae* in industrial applications. Here, we describe genetic tools for genome editing and breeding *K. marxianus* strains, which we use to create a new thermotolerant strain with promising fatty acid production.

These results open the door to using *K. marxianus* as a versatile synthetic biology platform organism for industrial applications.

KEYWORDS CRISPR-Cas9, *Kluyveromyces marxianus*, lipogenesis, mating, renewable chemicals, thermotolerant yeast

Synthetic biology is used to harness the metabolic capacity of microorganisms for the biosynthesis of simple and complex compounds now sourced unsustainably from fossil fuels or that are too expensive to make using chemical synthesis at industrial scale. The yeast *Saccharomyces cerevisiae* has served as the major eukaryotic organism for synthetic biology, but lacks the metabolic potential that could be exploited in many of the more than one thousand yeast species that have been identified to date. These yeasts remain difficult to use, however, as there are few synthetic biology tools to access their underlying metabolic networks and physiology (1). The budding yeast *Kluyveromyces marxianus* possesses a number of beneficial traits that make it a promising alternative to *S. cerevisiae*. *K. marxianus* is the fastest-growing eukaryotic organism known (2), is thermotolerant, growing and fermenting at temperatures up to 52 and 45°C, respectively (3), and uses a broad range of carbon sources, including pentose sugars. These traits are polygenic and would be difficult to engineer into a less robust host such as *S. cerevisiae*. *K. marxianus* also harbors high strain-to-strain physiological and metabolic diversity, which could prove advantageous for combining beneficial traits by sexual crossing. However, *K. marxianus* is generally found to be homothallic (4, 5) (i.e., is self-fertile) and cannot be crossed in a controlled manner.

For *K. marxianus* to be useful as a yeast platform for synthetic biology, it will be essential to establish efficient gene editing tools along with methods to cross strains with stable ploidy. These tools would enable rapid strain development, by generating genetic diversity and facilitating stacking of industrially important traits. The CRISPR-Cas9 (clustered regularly interspaced short palindromic repeats with Cas9) gene editing system has been used in many yeasts, including *S. cerevisiae*, *Schizosaccharomyces pombe*, *Yarrowia lipolytica*, *Kluyveromyces lactis*, and recently *K. marxianus* (6–9). Genome editing in *K. marxianus* should allow manipulation of known genetic targets. However, most desired traits likely depend on multiple, unlinked genetic loci, which remain difficult to identify without the ability to carry out genetic crosses. The ability to cross phenotypically diverse *S. cerevisiae* strains has been an indispensable tool for exploring its biology on a genome-wide scale and for improving its use as an industrial host (10). To approach the versatility of *S. cerevisiae* genetics, it will be necessary to gain full control over *K. marxianus* ploidy and mating type. As a homothallic yeast, *K. marxianus* lacks a permanent mating type, because *K. marxianus* haploid cells naturally change their mating type (either the **a** mating type, *MAT***a**, or α mating type, *MAT*α) leading to uncontrolled *MAT***a**/*MAT*α diploidization within a population (11). This stochastic ploidy makes it impossible to carry out quantitative biological studies of interesting traits that are ploidy specific (12), as it leads to populations with mixed phenotypes and prevents *K. marxianus* domestication through selective crossing.

To overcome the limitations in using *K. marxianus* as a synthetic biology platform, we adapted the CRISPR-Cas9 system we developed for *S. cerevisiae* (13) for use in *K. marxianus*, enabling both nonhomologous end joining (NHEJ) and homology-directed repair (HDR)-based genome editing. We identified the genetic loci responsible for mating-type switching in *K. marxianus* and created domesticated laboratory strains by simultaneously inactivating these genes. With this platform in place, we explored a large collection of wild *K. marxianus* strains to investigate *K. marxianus* lipid production at high temperatures. By domesticating and crossing promising strains, we were able to combine three complex traits—the ability to take up exogenous DNA (transformability), thermotolerance, and higher lipid production—into single *K. marxianus* isolates.
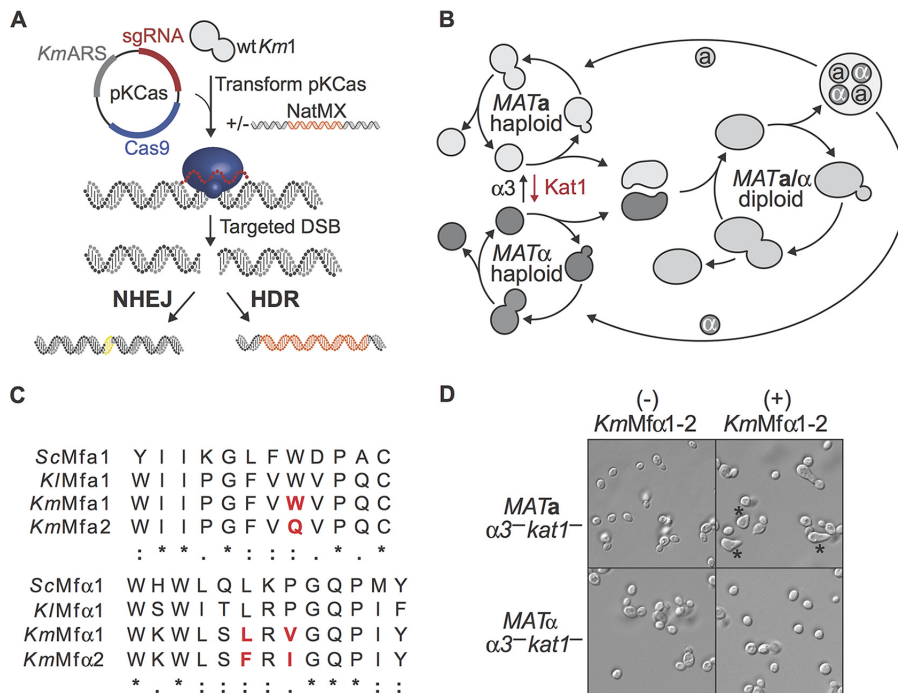
FIG 1 CRISPR-Cas9 genome editing and mating-type switching in *K. marxianus*. (A) CRISPR$_{NHEJ}$ and CRISPR$_{HDR}$ systems. *K. marxianus* transformed with the pKCas plasmid generates small indels near the cut site, a common product of nonhomologous end joining (NHEJ) repair of the DNA double-strand break. When transformed with both the pKCas plasmid and a donor DNA, homologous recombination products are seen in the target site. (B) Yeast life cycle. Haploid *MATa* and *MATα* switch mating type by transposases α3 and Kat1 in *K. lactis*. Haploid cells conjugate to form *MATa*/*MATα* diploids. Diploids undergo meiosis to form haploid spores that germinate to complete the life cycle. (C) Mature **a**- and α-pheromones from *K. marxianus* aligned with the *S. cerevisiae* and *K. lactis* sequences. Red indicates nonconserved amino acids between *K. marxianus* **a**- and α-factors. Amino acids are marked as identical (*), with similar polarity (:), or with different polarity (.). (D) Incubation of putative heterothallic *MATa* and *MATα* strains with a cocktail of both mature α-factor pheromones (*Km*Mfα1 and -2) results in mating projections from the *MATa* strain only (*).

RESULTS

CRISPR-Cas9 system in *K. marxianus*. We established robust genome editing in *K. marxianus* by adapting the plasmid-based CRISPR-Cas9 (CRISPRm) system we previously developed for *S. cerevisiae* (13). We first identified a *K. marxianus*-specific origin of replication and *K. marxianus*-specific promoters and terminators for expressing Cas9 (see Materials and Methods). We used the *S. cerevisiae* gene for tRNA^{Phe} as an RNA polymerase III promoter to express single-guide RNAs (sgRNAs) from the same plasmid (Fig. 1A). To test the effectiveness of the redesigned CRISPR-Cas9 system, we used a wild strain we isolated from a sugarcane bagasse pile (Km1 [Table 1]), and a Km1-derived *MATa* heterothallic strain (Km30 [see Table S1 in the supplemental material]). We transformed the pKCas plasmid (G418^R) carrying an sgRNA targeting the *URA3* gene into Km1, plated on G418 plates, and then selected for 5-fluoroorotic acid (5-FOA) resistance by replica plating to identify *ura3*$^-$ colonies. The efficiency of NHEJ-based Cas9 editing (CRISPR$_{NHEJ}$)—the number of *ura3*$^-$ colonies divided by the number of total G418^R transformants—was near 90% and was confirmed by sequencing the *URA3* locus. Targeting other genes across the genome resulted in around 75% efficiency (see Fig. S1 in the supplemental material). To test the ability of the *K. marxianus* CRISPR system to insert exogenous DNA at a defined locus, we also cotransformed into strain Km30 the pKCas plasmid encoding a guide RNA targeting the *URA3* gene along with a double-stranded DNA repair template comprised of a linear nourseothricin resistance cassette flanked by *K. marxianus URA3* homology sequences adjacent to the Cas9 target site (NatMX flanked by 0.9-kb homology arms). Using replica plating of G418^R trans-

TABLE 1 List of wild-type *K. marxianus* strains used in this work

Strain[a]	Designation no. by:			
	ATCC	NCYC	CBS	NRRL
Km1				
Km2	10022	100	6432	Y-665
Km5	46537	851	397	Y-2415
Km6		143	608	Y-8281
Km9	26548	2597	6556	Y-7571
Km11	36907	587		
Km16	10606		396	Y-1550
Km17	8635/28910			Y-1190
Km18			1089	Y-2265
Km19	26348			
Km20				
Km21				

[a]Km1, Km20, and Km21 were isolated from sugarcane bagasse piles. Km1 was isolated at Raceland Raw Sugar Corporation, Raceland, LA. Km20 and Km21 were isolated at the Sugarcane Growers' Cooperative, Belle Glade, FL.

formants onto two selection plates—5-FOA to detect *ura3*⁻ alleles and Nat^R to detect HDR events—we found 100% of the colonies to be *ura3*⁻ and ~97% (189/195) to be Nat^R, indicating that repair of Cas9-induced double-strand breaks allowed highly efficient HDR-mediated gene integration (CRISPR$_{HDR}$). We used colony PCR on select Nat^R colonies (targeting outside the 0.9-kb homology arms of the NatMX cassette) to confirm NatMX cassette integration at the *URA3* locus.

Engineering mating-competent heterothallic *K. marxianus* strains. We used CRISPR$_{NHEJ}$ to make stable *K. marxianus* laboratory strains with defined ploidy and mating type to enable the use of classical yeast genetics. Most naturally isolated *K. marxianus* strains are homothallic: i.e., they change their mating type spontaneously by "mating-type switching" to create mixed populations of *MAT***a**, *MAT*α, and *MAT***a**/*MAT*α cells (4, 5). The *K. marxianus* mating-type switching mechanism is not genetically conserved with the well-characterized HO endonuclease mechanism employed by *S. cerevisiae*. Notably, a two-component switching mechanism has been identified in *Kluyveromyces lactis* (14, 15), which uses two transposases (Kat1 and α3) for *MAT* switching. The α3 transposase switches *MAT*α type cells to *MAT***a** type, and Kat1 switches *MAT***a** to *MAT*α type (Fig. 1B).

We identified the *K. marxianus* orthologs of the *K. lactis KAT1* and *ALPHA3* genes using reciprocal BLASTp against predicted open reading frames (ORFs) from the whole-genome sequence of Km1 (see Table S2 in the supplemental material) (16). Using CRISPR$_{NHEJ}$, we targeted both transposase genes (Table S2) to create frameshift mutation loss-of-function alleles. We then isolated several of these double-transposase-inactivated Km1 α3⁻ *kat1*⁻ strains that had small base pair insertions or deletions near the Cas9 cut site (Fig. S1). To identify *MAT***a** haploid isolates, we used a pheromone morphological response assay. Yeast mating is initiated by the secretion of small peptide pheromones **a**-factor and α-factor by *MAT***a** and *MAT*α cells, respectively. The pheromones, derived from **a**-pheromone and α-pheromone precursor proteins, m̲ating f̲actor **a̲** (MFA1 and MFA2) and m̲ating f̲actor α̲ (MFα1), are detected by their cognate cell surface recognition proteins and lead to polar morphogenesis or the formation of mating projections ("shmoo") that can be used to deduce a strain's mating type. We identified two putative *K. marxianus MFA* genes (*KmMFA1* and *KmMFA2*) as well as the *MF*α gene (*KmMFα1*, encoding two isotypes, *Km*MFα1 and *Km*MFα2) in the *K. marxianus* genome by reciprocal BLASTp using the *S. cerevisiae* and *K. lactis* protein sequences as queries (16, 17) (Fig. 1C; see Fig. S2A in the supplemental material). Incubation of *K. marxianus* strain Km1 α3⁻ *kat1*⁻ cells with synthetic *Km*MFα1 and *Km*MFα2 peptide pheromones resulted in isolates that responded to both α-factors (Fig. 1D), indicating these are *MAT***a** α3⁻ *kat1*⁻ haploids. We categorized unresponsive strains as either *MAT*α or diploid strains, using sequencing of the *MAT* locus (Fig. S2B).

Once we identified stable *MAT***a** α3⁻ *kat1*⁻ or *MAT*α α3⁻ *kat1*⁻ strains through the pheromone response method and subsequent sequencing of the *MAT* locus (Table S2
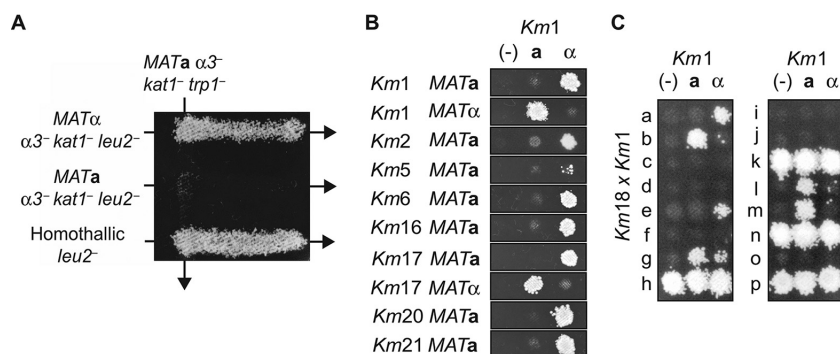
FIG 2 Creation of heterothallic *K. marxianus* strains. (A) Auxotrophic mating assay of Km1 strains. Shown are results from strains Km1 *MATα α3⁻ kat1⁻ leu2⁻*, Km1 *MATa α3⁻ kat1⁻ leu2⁻*, and homothallic Km1 *leu2⁻*, streaked through strain Km1 *MATa α3⁻ kat1⁻ trp1⁻* on 2% glucose plates and replica plated onto SCD − (Leu, Trp) plates after 2 days. Diploid growth is seen only upon sexual crossing between strains with opposite mating types or with homothallic haploid strains. (B) Auxotrophic mating assay of several *α3⁻ kat1⁻ leu2⁻* triple-inactivation strains and Km1 *MATa α3⁻ kat1⁻ trp1⁻* or Km1 *MATα α3⁻ kat1⁻ trp1⁻*. Putative heterothallic strains were spotted over the negative control (−), the Km1 *MATa α3⁻ kat1⁻ trp1⁻* reference (a), or the Km1 *MATα α3⁻ kat1⁻ trp1⁻* reference (α) on glucose plates for mating. Replica plating onto SCD − (Leu, Trp) results in diploid growth. (C) The wild homothallic isolate Km18 was made *trp⁻* by UV mutagenesis and crossed with heterothallic *Km*1 *MATa α3⁻ kat1⁻ leu2⁻*. Diploids were sporulated, 16 spores were isolated (a through p) and germinated, and the resulting haploids were screened for heterothallic strains by crossing with Km1 *MATa α3⁻ kat1⁻ trp1⁻* or Km1 *MATα α3⁻ kat1⁻ trp1⁻*. Screened haploids were auxotrophic strains unable to mate (c, d, f, i, j, and o), possible *trp⁻* revertants (h, k, n, and p), homothallic (g), or heterothallic (a, b, e, l, and m).

and Fig. S2B), we tested for the ability of two haploid strains with different auxotrophic markers to mate and form prototrophic diploids. First, we used CRISPR$_{NHEJ}$ to create *leu2⁻* or *trp1⁻* auxotrophic mutants of the predicted heterothallic *MATa α3⁻ kat1⁻* and *MATα α3⁻ kat1⁻* or *MATa/MATα* strains. Then, *MATa α3⁻ kat1⁻ trp1⁻* and *MATα α3⁻ kat1⁻ leu2⁻* strains were combined by opposing streaks on mating-inducing medium. After 2 days, successful mating of *MATa α3⁻ kat1⁻ trp1⁻* and *MATα α3⁻ kat1⁻ leu2⁻* cells resulted in growth when cells were replica plated onto minimal medium lacking tryptophan and leucine (Fig. 2A). To test whether the engineered heterothallic strains could still mate with homothallic wild-type isolates, heterothallic Km1 *MATa α3⁻ kat1⁻ trp1⁻* cells were streaked with the homothallic haploid Km1 *leu2⁻* strain, resulting in mating and diploid growth (Fig. 2A). These data confirm the CRISPR$_{NHEJ}$-engineered Km *α3⁻ kat1⁻* strains are heterothallic and result in stable haploid, breeding-competent isolates that can mate with opposite mating types and wild homothallic strains.

To further validate the role of α3 and Kat1 in switching mating types, we performed complementation assays by constitutively expressing these transposases from plasmids. Plasmids encoding Kat1 or α3 were transformed into Km1 *α3⁻ kat1⁻ leu2⁻* strains to revert the controlled mating phenotype and promote homothallism. Transformants were then tested for mating-type switching by crossing them with stable heterothallic reference strains (*α3⁻ kat1⁻ trp1⁻*) of either *MATa* or *MATα* mating type. Using the auxotrophic mating assay, these experiments showed that complementing stable *MATa* mutants with Kat1 overexpression plasmids or stable *MATα* mutants with α3-expressing plasmids induced mating-type switching. Kat1 caused *MATa* isolates to switch and mate with a *MATa* reference strain, and α3 caused *MATα* isolates to switch and mate with a *MATα* reference strain (see Fig. S3 in the supplemental material).

A strong advantage of turning *K. marxianus* into a synthetic biology chassis for metabolic engineering is its high strain-to-strain phenotypic and metabolic diversity (18). To build a widely useful yeast platform, we sought to create heterothallic strains of each mating type for 12 wild isolates collected from the ATCC and CBS culture collections and our own isolates (Table 1). These strains have been isolated from diverse locations and substrates around the world, from dairy to sugarcane bagasse. We used CRISPR$_{NHEJ}$ to create strains with inactivation of three genes: those encoding the transposases Kat1 and α3 and an auxotrophic marker, either *TRP1* or *LEU2*. Triple-
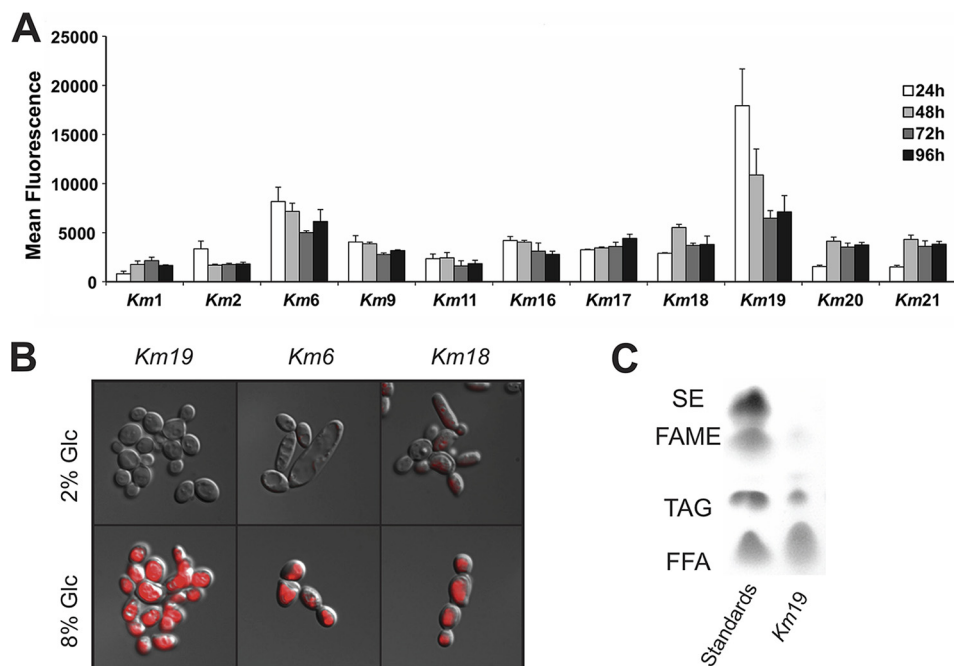
FIG 3 Lipogenesis of *K. marxianus* strains. (A) Nile red fluorescence flow cytometry of 11 wild-type isolates after 24, 48, 72, and 96 h at 42°C in lipogenesis medium. Experiments were carried out in biological triplicate, with means and standard deviations shown. (B) DIC images superimposed with epifluorescence microscopy of Nile red-stained cells. Little or no fluorescence is seen after 24 h in 2% glucose. After 24 h in 8% glucose at 42°C (Km19 and Km6) and 48 h (Km18), fluorescence is seen encompassing the majority of the cell volume. (C) TLC analysis of Km19 total lipids after 24 h in 8% glucose at 42°C. Lane 1, ladder of standards containing steryl ester (SE), fatty acid methyl ester (FAME), triacylglycerols (TAG), and free fatty acids (FFA). Lane 2, Km19 lipids.

inactivation strains ($\alpha3^-$ $kat1^-$ $leu2^-$ or $\alpha3^-$ $kat1^-$ $trp1^-$) were successfully isolated from 10 of the isolates. We assayed these strains for mating type by crossing them with heterothallic Km1 strains as a reference, using the auxotrophic mating assay described above. Heterothallic haploids (*MAT***a** and/or *MAT*α) were isolated from 10 of the triple-inactivation strains (Fig. 2B). For strain Km18, which was difficult to transform with plasmid DNA, stable heterothallic strains could be isolated from a cross between a homothallic Km18 strain first made trp^- using UV mutagenesis and Km1 heterothallic strains. The Km18 trp^- × Km1 diploids were sporulated and germinated and then back-crossed with Km1 haploid reference strains to establish their mating type (Fig. 2C).

K. marxianus strains engineered for higher levels of lipogenesis. To explore the industrial potential of *K. marxianus* compared to *S. cerevisiae* (i.e., thermotolerance and Crabtree-negative growth, preferring respiration over fermentation [19]), we tested lipid production in *K. marxianus* under aerobic conditions. We first screened 11 wild-type *K. marxianus* isolates for levels of lipogenesis using a lipophilic fluorescent dye (Nile red), combined with flow cytometry and cell sorting. Nile red localizes to lipid droplets in yeast and exhibits increased red fluorescence proportional to the total amount of lipid in the cell (20, 21). The *K. marxianus* strains were grown in 8% glucose or 8% cellobiose lipogenesis medium at 30 and 42°C, and time point samples were collected every 24 h to be analyzed by flow cytometry. The highest fluorescence was observed in strains fed 8% glucose at 42°C for 24 h, with large strain-to-strain differences spanning an ~20-fold change in fluorescence (Fig. 3A). A few strains also produced significant amounts of lipid in cellobiose at 42°C, compared to their production of lipid in glucose (i.e., strains Km2 and Km17 [Table 1]) (see Fig. S4A in the supplemental material). All strains produced much lower levels of lipid when grown at 30°C.

We used fluorescence microscopy to examine the cell morphology of the strains with the highest lipid titers. When Nile red fluorescence was overlaid with differential interfer-
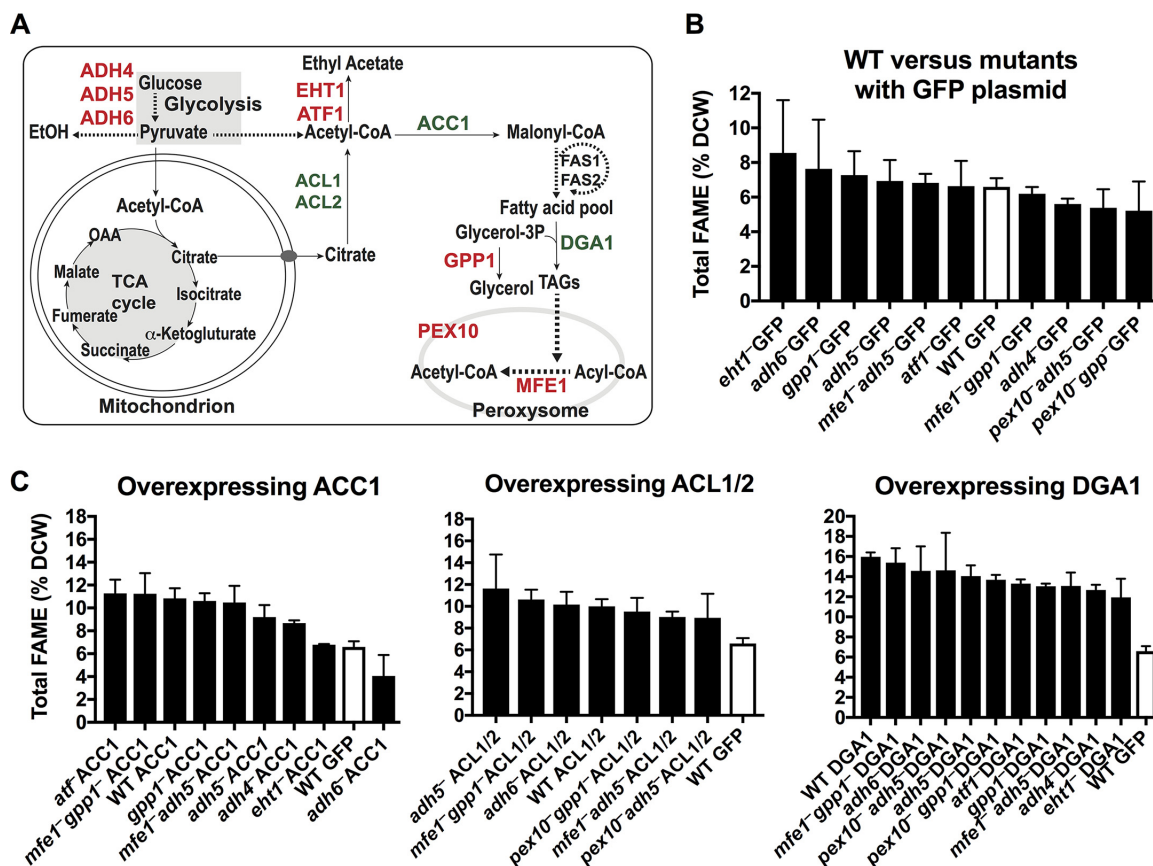
FIG 4 Genetic dissection of lipogenesis of a high-producing *K. marxianus* strain, Km6. (A) General overview of lipid-related metabolism. Genes in red were inactivated with CRISPR$_{NHEJ}$, and genes in green were overexpressed using plasmids. (B) Percentage of fatty acids in dry cell weight (DCW) after 24 h under lipogenic conditions at 42°C for several variants of Km6 (wild type and mutants). (C) Percentage of fatty acids in dry cell weight for several Km6 variants containing *ACC1*, *DGA1*, and *ACL1/2* overexpression plasmids. In panels B and C, all experiments were carried out in biological triplicate, with mean values and standard deviations shown. Lipogenesis medium in panels B and C contained monosodium glutamate instead of ammonium sulfate.

ence contrast (DIC) images of *K. marxianus* isolates Km19, Km6, and Km18 (Table 1) after 24 or 48 h of growth in 8% glucose at 42°C, large lipid droplets encompassed a large fraction of the cell volume (Fig. 3B). Km19 produced the highest levels of lipids as measured by Nile red fluorescence, which peaked after only 24 h (Fig. 3A), at which point Km19 had accumulated lipids at ~10% dry cell weight (Fig. S4B). Thin-layer chromatography (TLC) revealed that the majority of the lipid in Km19 accumulated as free fatty acids (FFAs) (Fig. 3C).

Strain engineering for higher lipid production. Lipogenesis in oleaginous yeasts such as *Yarrowia lipolytica* results in the synthesis and storage of lipid droplets within the cytoplasm (22). Lipid biosynthesis is largely dependent upon the enzymes AMP deaminase (AMPD), ATP-citrate lyase (ACL), acetyl coenzyme A (acetyl-CoA) carboxylase (ACC), and malic enzyme (MAE) (23). Collectively, these enzymes promote the accumulation of acetyl-CoA via citrate. Interestingly, although ACL is thought to be crucial for lipogenesis in oleaginous yeasts (24), we did not identify the genes *ACL1* and *ACL2* in the *K. marxianus* reference strain, Km1. ACC1 then converts acetyl-CoA into malonyl-CoA, and the malic enzyme provides NADPH, the reduced cofactor necessary for the production of lipids. Total lipid accumulation is a balance between lipid synthesis and catabolism through β-oxidation in the peroxisome (Fig. 4A). Engineered strains of *Y. lipolytica* with reduced β-oxidation (*pex10Δ*) and peroxisome biogenesis (*mfe1Δ*) combined with overexpression of lipogenesis enzymes can store up to 80 to 90% dry cell weight as lipid compared to only ~10 to 15% lipid content for wild-type cells (23).

However, the high yield of lipogenesis in *Y. lipolytica* often takes up to 5 days to reach its peak (25) and requires temperatures of ~30°C, due to the lack of thermotolerance in this yeast (23).

We tested whether inactivation or overexpression of genes previously shown in *Y. lipolytica* to contribute to high lipid production (23) would affect the ability of *K. marxianus* to produce lipids. Although wild-type Km19 produced the most lipids of the wild-type strains we tested, Km19 is very difficult to transform with plasmids. Therefore, we chose to use strain Km6 (Table 1), since it has similar lipid content and is easily transformed with plasmid DNA, allowing the facile use of plasmid-based CRISPR-Cas9 to inactivate genes or plasmid-based overexpression.

Unlike *Y. lipolytica*, fermentation of glucose to ethanol and esterification of acetate to ethyl acetate are likely to compete with lipogenesis in *K. marxianus*. Therefore, we inactivated genes by CRISPR$_{NHEJ}$ to decrease ethanol fermentation (*ADH* genes) (26) and ethyl acetate production (*ATF* genes) (7), as well as ester biosynthesis (*EHT1*) (7, 27) and glycerol biosynthesis (*GPP1*). We also inactivated genes involved in β-oxidation (*PEX10* and *MFE1*) (23) (Fig. 4A). For the overexpression experiments, we cloned genes known to be involved in the accumulation of lipids (*DGA1*, *ACC1*, and the dimer *ACL1/ACL2*) into overexpression plasmids constructed using strong promoters (*KmTDH3* or *KmPGK1*) to drive the expression of these genes. The plasmids were individually transformed into wild-type Km6 or strains in which CRISPR$_{NHEJ}$ had been used for targeted gene inactivation. The fatty acid content of each of these engineered strains was measured by gas chromatography and calculated as the percentage of dry cell weight. Although none of the inactivated genes had an appreciable effect on the accumulation of fatty acids (Fig. 4B), overexpression of *DGA1* increased the levels of fatty acids across all strains tested, more than doubling the fatty acid content in the wild-type strain (Fig. 4C). No appreciable differences were found in terms of the fatty acid composition, except for the Km6 *eht1*⁻ strain bearing the *ACC1* plasmid, which had more than 80% of its total fatty acids comprised of stearic acid (18:0), compared to ~10 to 20% in the other strains (see Fig. S5 in the supplemental material).

Breeding to isolate high-producing, thermotolerant, and transformable strains. The ability to cross phenotypically diverse and stable haploid *K. marxianus* strains should enable combining several beneficial traits into a single strain. For example, strain Km19 is the best lipid-producing strain we identified (Fig. 3A), but it is neither easily transformed nor thermotolerant compared to other *K. marxianus* strains. On the other hand, strain Km17 transforms easily and is thermotolerant (growing at 45°C) but is only moderately oleaginous (Fig. 3A). We therefore crossed these two strains to combine their beneficial traits into single isolates. We first engineered Km19 *α3*⁻ *kat1*⁻ *trp1*⁻ using CRISPR$_{NHEJ}$ and crossed a *MAT***a** isolate with an engineered stable haploid Km17 *MATα α3*⁻ *kat1*⁻ *leu2*⁻ strain. The resulting diploids were sporulated and then germinated at high temperature (44°C) to select for thermotolerant segregants, and 91 haploid progeny were picked to screen for lipid production and plasmid transformability (Fig. 5A).

Single segregants isolated from the above temperature selection were individually scored in terms of lipid production using Nile red staining and flow cytometry and displayed high variability in lipid production (see Fig. S6 in the supplemental material). A few segregants performed better than the parental Km19 haploid strain, but a number of these had high fluorescence due to aggregation, as determined by light microscopy, and were therefore excluded from further analysis. Strains that did not aggregate had their fatty acid percentage in dry cell weight and composition measured using gas chromatography-flame ionization detection (GC-FID) (Fig. 5B). Notably, three of these isolates produced lipids as well as the parent Km19 strain, while inheriting the thermotolerance and transformability of Km17 (Fig. 5C and D; see Fig. S7 in the supplemental material). These strains therefore combined all three beneficial traits of the parental strains.
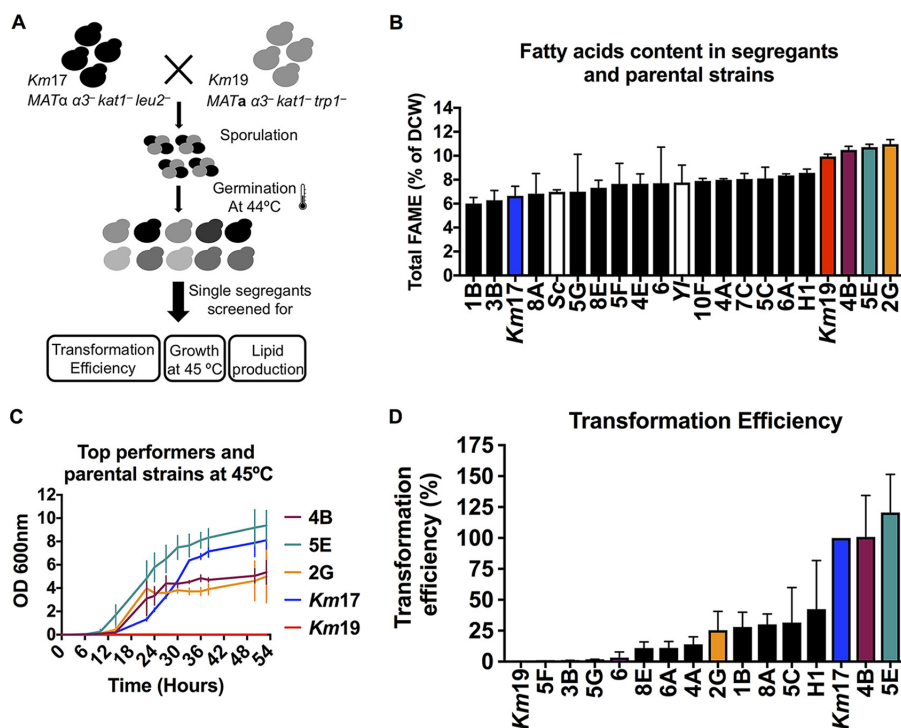
FIG 5 Selection of *K. marxianus* strains with combined beneficial traits. (A) Selection strategy. Km19 and Km17 were crossed, sporulated, and then germinated at 44°C to select for thermotolerant segregants. Single segregants were isolated and tested for lipid production, transformability, and high-temperature growth. (B) Fatty acid percentage in dry cell weight (DCW) for several segregants from the Km17 × Km19 cross and the parental strains. Three segregants have similar profiles to the more lipogenic parental strain (Km19). Experiments are from biological triplicates with mean and standard deviation shown. (C) Growth curves at 45°C for the segregants 4B, 5E, and 2G, as well as parental strains Km17 and Km19, in biological triplicate. Km19 is unable to grow at this temperature. Growth curves for parental strains at 30, 37, and 42°C can be found in the supplemental material (Fig. S7A), as well as for segregants at 30 and 37°C (Fig. S7B). (D) Transformation efficiency for several segregants normalized by Km17 transformation efficiency. Experiments are from 2 to 4 biological replicates with normalized mean and standard deviations shown.

DISCUSSION

Common metabolic engineering techniques are not ideal when dealing with complex phenotypes such as thermotolerance, productivity, and robustness (28). Therefore, agnostic approaches for combining complex traits into model yeast species are of high value, including directed evolution (29), genome-wide transcriptome engineering (30), and genome shuffling (31). However, these cannot substitute for classical sexual crossing for combining strain-specific traits. It is known that sexual reproduction enables adaptation to stressful industrial environments due to the faster unlinking of deleterious allelic pairs compared to clonal populations (10). Here we establish *K. marxianus* as a platform for synthetic biology by engineering stable heterothallic haploid strains that can be crossed to combine complex, unmapped multigenic traits into one strain.

In *S. cerevisiae*, inactivation of a single gene encoding HO endonuclease makes this yeast heterothallic and is sufficient to gain laboratory control of its mating cycle (32). While inactivation of the single transposase α3 can be used to cross *K. marxianus* strains (8), the resulting strains possess unstable mating types due to the presence of Kat1 and could randomly switch from *MAT***a** to *MAT*α (Fig. 1B and Fig. 2C; Fig. S3). To establish stable crossing in *K. marxianus* and abolish self-mating, we used CRISPR$_{NHEJ}$ to inactivate both transposases that are responsible for mating-type switching (α3 and Kat1) (Fig. 1B). By simultaneously inactivating *ALPHA3* and *KAT1*, we created stable heterothallic α3⁻ kat1⁻ strains that cannot switch mating type and, therefore, can be mated in a controlled manner with strains of the opposite mating type (Fig. 2A; Fig. S3).

Alternative methods for creating stable haploids by deleting the silenced *MAT* loci have been used in yeast (33), but this strategy creates sterile strains and can be lethal if the endonuclease that initiates the double-strand break required for mating-type switching is not inactivated as well (34). Our strategy of inactivating both the α3 and Kat1 transposases preserves the ability to mate *K. marxianus* strains, an essential tool for synthetic biology, and to take advantage of this yeast's remarkable phenotypic diversity. We successfully isolated heterothallic haploid strains from 12 wild-type isolates. These strains readily mate with each other, resulting in sporulation-competent diploids that segregate to viable haploid spores. Combined with CRISPR-Cas9 genome editing (Fig. 1) (6–9), these results establish a full set of tools for use of *K. marxianus* as a synthetic biology host and for future exploration of its biology on a genome-wide scale.

Using both sets of synthetic biology tools described here, we sought to exploit the diversity of *K. marxianus* as a thermotolerant, fast-growing, Crabtree-negative yeast. Screening 11 of the wild-type isolates for high levels of lipogenesis, we found high strain-to-strain variability in lipid production. Notably, strain Km19 produced ~10% lipid by dry cell weight after 24 h at 42°C, a considerably shorter time than the 120 h required by wild-type *Y. lipolytica* to accumulate a similar amount of lipid (25). We find Km19 stores the vast majority of lipid as free fatty acids (FFAs) (Fig. 3C), in contrast to *Y. lipolytica*, which stores lipids as triacylglycerols (22, 35). FFAs are particularly suitable for the production of alkanes/alkenes and fatty alcohols, two types of high-value chemicals (36, 37). Although Km19 produces lipids at a high rate, it is not thermotolerant compared to other *K. marxianus* isolates (Fig. 5C) and is difficult to transform with plasmid DNA (Fig. 5D). To eliminate these barriers to conducting genetic engineering in the oleaginous strain Km19, we crossed it with Km17, which transforms well and grows well at 45°C. Notably, some progeny of this cross isolated as single segregants produced lipids to the same level of the parent Km19 strain while retaining thermotolerance and transformability of Km17 and were also not prone to aggregation. The power of combining multiple complex and valuable traits using stable heterothallic strains, together with CRISPR-Cas9 genome engineering, opens a new frontier to use *K. marxianus* as both a thermotolerant model species and an industrially relevant host.

MATERIALS AND METHODS

Strains, media, and culture conditions. The *K. marxianus* strains used in this study were purchased from ATCC (American Type Culture Collection) or CBS (The Dutch Centraalbureau voor Schimmelcultures, Fungal Biodiversity Centre) or were obtained from an in-house collection. A complete list of all the wild-type strains is given in Table 1. Strains Km1, Km20, and Km21 have internal identity codes YST31, 1S300000, and 1S1600000, respectively. Strains were stored at −80°C in 25% glycerol. All experiments began by inoculation of a 12-ml culture tube containing 3 ml yeast extract-peptone-dextrose (YPD) or synthetic complete dextrose (SCD) medium with a single colony grown on a YPD medium agar plate. Cultures were shaken at 250 rpm. YPD agar consisted of 10 g/liter yeast extract, 20 g/liter peptone, 20 g/liter glucose, and 20 g/liter agar. SCD consisted of 2 g/liter yeast nitrogen base (YNB) without amino acids or ammonium sulfate, 1 g/liter complete supplement medium (CSM), and 5 g/liter (NH$_4$)$_2$SO$_4$. Five percent malt extract medium was made by mixing 30 g of malt extract with 20 g of agar and bringing the volume to 1 liter with H$_2$O and then was sterilized by autoclaving at 10 lb/in^2 for 15 min. Sporulation (SPO) medium was made with 10 g/liter potassium acetate, 1 g/liter Bacto yeast extract, and 0.5 g/liter glucose. 5-FOA plates contained 2 g/liter yeast nitrogen base without amino acids or ammonium sulfate, 5 g/liter (NH$_4$)$_2$SO$_4$, 1 g/liter complete CSM, 20 g/liter glucose, 20 g/liter agar, and 1 g/liter 5-fluoroorotic acid (5-FOA). Lipogenesis medium contained 2 g/liter YNB without amino acids and ammonium sulfate, 1 g/liter ammonium sulfate or monosodium glutamate, and 8% glucose or cellobiose.

Genome sequencing and annotation. A single-colony isolate of strain YST31 (Km1 [Table 1]) grown on a YPD plate was used to inoculate a YPD liquid culture and prepare genomic DNA using the YeaStar genomic DNA kit (Zymo Research). We submitted ~5 mg of genomic DNA for small insert library preparation (~250 bp) and Illumina sequencing. Library preparation and genome sequencing (Illumina HiSeq 2500) were performed by the UC Davis Genome Center DNA Technologies Core (http://dnatech.genomecenter.ucdavis.edu/). For YST31, we obtained 14,790,917 PE100 paired-end reads, and after trimming, we assembled reads into 116 scaffolds using CLC Genomics Workbench version 7.5.1. Default settings were used for quality trimming and *de novo* assembly. The median coverage was 250-fold, and the total genome assembly was 10,784,526 bp. Genome annotation was performed using an automated software pipeline, FGENESH++ (http://www.softberry.com) version 3.1.1. Genes were first predicted *ab initio* using FGENESH and then refined based on protein homology (38, 39). A custom BLAST database based on GenBank nr (downloaded 31 October 2014) was used for homology refinement of gene models. Gene prediction parameters were obtained from Softberry and were based on *Saccharomyces cerevisiae*

gene models as the training set. The resulting annotation output files were renumbered and converted into GenBank format using custom scripts provided by Softberry.

Cas9 plasmid construction. To manipulate *Kluyveromyces marxianus*, we created a plasmid that can replicate in both *Escherichia coli* and *K. marxianus* and confers resistance to kanamycin and Geneticin, respectively. We used plasmid pOR1.1 (13), which can replicate in *E. coli* and *S. cerevisiae*, as a backbone for further manipulation. We identified and cloned an autonomous replicating sequence (ARS) from commercially available *K. marxianus* strain ATCC 36907 (Km11 [Table 1]) as follows. Using a YeaStar genomic DNA extraction kit (Zymo Research, D2002), genomic DNA was extracted from *K. marxianus* ATCC 36907. One microgram of genomic DNA was incubated with restriction enzyme EcoRI (NEB, R0101S) to fragment the DNA. In parallel, the *S. cerevisiae* 2μ origin of replication was replaced with an EcoRI digestion site in pOR1.1. The plasmid was then linearized with EcoRI and treated with shrimp alkaline phosphatase (Affymetrix, 78390) to dephosphorylate the DNA ends and prevent religation of the vector. The genomic DNA fragment pool was ligated with the linearized plasmid using T4 DNA ligase (Invitrogen, 15224017), transformed into One Shot TOP10 competent *E. coli* (C404003), and plated on kanamycin selection plates. All growing colonies were pooled, and the plasmids were extracted using the QIAprep spin miniprep kit (Qiagen, 27106). Two micrograms of the resultant plasmid pool was transformed into ATCC 36907 and plated on Geneticin selection plates. Many colonies were picked, and plasmid extraction was performed for each using the Zymo Research yeast plasmid extraction kit (D2001). The plasmids were individually transformed back into One Shot TOP10 competent *E. coli*, and the plasmids were extracted once more and digested with EcoRI. The digests were run on a 1% agarose gel with TAE (Tris-acetate-EDTA) buffer (40), and the clone with the smallest insert was chosen. The insert was sequenced and then systematically trimmed to a 232-bp functional region that still conferred the ability of the plasmid to replicate in *K. marxianus* (Table S2).

The resulting plasmid with a *K. marxianus* ARS was then modified to express Cas9 and a single-guide RNA (sgRNA) cassette using transcription promoters and terminators from *K. marxianus*. The *S. cerevisiae* promoter and terminator for Cas9 as used in pCas (13) were replaced with those for homologous genes in *K. marxianus*. In the new plasmid, Cas9 expression was driven by the promoter region of the gene *KmRNR2*—a mild-strength promoter—and terminated by the strong *KmCYC1* terminator. *S. cerevisiae* tRNAs were used as promoters to drive sgRNA expression (13) and terminated by the *S. cerevisiae SNR52* (*ScSNR52*) terminator. Between the promoter and the sgRNA, there is a hepatitis δ-ribozyme sequence that cleaves off the 5' leader sequence, liberating the tRNA from the sgRNA body that binds to Cas9 protein. The released transcript contains the δ-ribozyme, the protospacer sequence that targets Cas9 to the desired sequence, and the scaffold sgRNA (13).

Overexpression plasmid construction. Four genes found to be involved in lipogenesis in other yeasts were cloned into overexpression plasmid backbones using the In-Fusion cloning kit (Takara). The cloning reaction mixtures contained 25 to 50 ng of vector, 3 times molar excess of PCR-generated insert, and 0.5 μl of In-Fusion in a final volume of 2.5 μl. *K. marxianus* ACC1 and DGA1 coding sequences were amplified from Km6 gDNA using Phusion polymerase and cloned into two different linearized backbones, while *Yarrowia lipolytica* ACL1 and ACL2 coding sequences were cloned into the same plasmid. The vector backbone was the same used for pKCas9 construction, containing a *K. marxianus* ARS isolated as described above, a Geneticin resistance marker, and the pUC bacterial origin of replication. ACC1 and ACL1 were controlled by the *K. marxianus* GK1 promoter, while DGA1 and ACL2 were under the control of the TDH3 promoter (Table S2). All ORFs were terminated by the *K. marxianus* CYC1 terminator sequence. The resulting plasmids were transformed into wild-type *K. marxianus* strain Km6 (Table 1), as well as into 10 knockout mutant strains derived from Km6 that were constructed using CRISPR$_{NHEJ}$: *adh5$^-$*, *adh6$^-$*, *adh4$^-$*, *gpp1$^-$*, *atf1$^-$*, *eht1$^-$*, *mfe1$^-$ gpp1$^-$*, *mfe1$^-$ adh5$^-$*, *pex10$^-$ gpp1$^-$*, and *pex10$^-$ adh5$^-$* (Table S1).

High-efficiency DNA transformation. We established a high-efficiency transformation protocol for *K. marxianus* as follows. A single colony was inoculated in 1.5 ml of YPD medium and incubated at 30°C overnight, then 180 μl of this culture was transferred to 5 ml of fresh YPD medium and incubated at 30°C until the optical density at 600 nm (OD$_{600}$) reached 1.0 to 1.2 (~5 to 6 h). Then, 1.4 ml of the culture was aliquoted into microcentrifuge tubes and spun down at 3,000 × *g* for 5 min. The supernatant was removed, and the pellet was resuspended in 50 mM lithium acetate, followed by incubation at room temperature for 15 min. The cells were spun down, the supernatant was discarded, and the cells were used for subsequent transformation reactions.

Single-stranded DNA (ssDNA) was previously prepared as follows (41): 2 μg/μl of ssDNA from Sigma (D1626-250mg) was agitated with a stir bar overnight in TE buffer (10 mM Tris [pH 8.0] and 1 mM EDTA) at 4°C and then concentrated to 10 μg/μl by isopropanol precipitation, resuspended in water, and quantified (NanoDrop 1000; Thermo Scientific). Prior to each transformation, aliquots of ssDNA were boiled for 5 min and then placed in an ice bath for 5 min. Keeping all the reagents on ice, 66.7 μl of 60% polyethylene glycol (PEG) 2050, 12.5 μl of 2 M lithium acetate, and water in a final volume of 100 μl were added to a sterile microcentrifuge tube. Then 2 μl of 1 M dithiothreitol (DTT) and 25 μg of ssDNA were added, followed by 0.1 to 5 μg of pKCas plasmid DNA. The transformation mixture was briefly vortexed, and 100 μl was added to the cells. The transformation reaction mixture was then incubated at 42°C for 40 min. The reaction was spun down for 5 min at 3,000 × *g*, the supernatant was removed, and 500 μl of fresh YPD was added. The cells were allowed to recover for 2 h at 37°C and 250 rpm. Then 10% of the volume was spread on a YPD G418 selection plate, and the remaining volume was spread on a second G418 plate.

CRISPR$_{NHEJ}$ and CRISPR$_{HDR}$. We transformed the pKCas plasmid into *K. marxianus* strains in the absence of donor repair DNA to determine the efficiency of NHEJ repair of the double-strand break. We cloned the guide sequence for the sgRNA in pKCas to target *URA3* (Table S2), to allow counterselection

with 5-fluoroorotic acid (5-FOA) plates, which select for *ura3⁻* colonies. Approximately 1 μg of pKCas plasmid was transformed into *K. marxianus*, and the efficiency of editing was calculated by counting the number of *ura3⁻* colonies divided by the number of G418^R transformants. Sequencing of the targeted region revealed small insertions or deletions (indels) around the Cas9 cleavage site typical of NHEJ, resulting in premature stop codons within the *URA3* ORF (Fig. S1). We find that this system can be used to create inactive alleles in different genes with efficiencies of ~75% (Fig. S1).

We modified the high-efficiency transformation protocol to enable cotransformation of the pKCas plasmid and a linear repair DNA template (donor DNA), for HDR-mediated genome editing. For tests of HDR-mediated gene insertion, the donor DNA targeted for genome integration contained the NatMX cassette conferring resistance to nourseothricin and 0.9 kb of flanking homology to the target site in the *K. marxianus* genome. Donor DNA was generated by PCR and concentrated by isopropanol precipitation (42). The best ratio of plasmid to donor DNA was 0.2 μg of pKCas plasmid and 5 μg of linear donor DNA, with 0.9 kb of homology to the Cas9 targeting site. Tests with higher concentrations of both pKCas and donor DNA were not as efficient. The transformation reaction was carried out as described above, except that cells were allowed to recover for 1 h at 37°C in YPD without drug at 250 rpm, after which G418 was added and the cells were allowed to recover overnight. For the nourseothricin gene insertion experiments, cells were plated on YPD G418 plates, incubated at 37°C overnight, and then replica plated on either 5-FOA or nourseothricin plates, to identify Nat^R colonies with correct insertion in the *URA3* locus. Colony PCR performed on select Nat^R colonies (targeting outside the 0.9-kb homology arms of the NatMX cassette) confirmed NatMX cassette integration at the *URA3* locus.

Mating-competent heterothallic strains. ALPHA3 and KAT1 double-inactivation strains (*α3⁻ kat1⁻*) were constructed using CRISPR$_{NHEJ}$ (Table S1). *K. marxianus* was transformed with either *KAT1*- or *ALPHA3*-targeting pKCas plasmids. Genomic DNA was isolated from G418^R colonies, the *KAT1* or *ALPHA3* regions were PCR amplified, and the PCR products were sequenced. Colonies with sequences containing indels that generated early stop codons were chosen and were saved as glycerol stocks. Single-inactivation strains were subjected to a second round of CRISPR$_{NHEJ}$ to inactivate the second transposase, creating the *α3⁻ kat1⁻* double mutants. These double mutants were then subjected to a third round of CRISPR$_{NHEJ}$ targeting the *LEU2* or *TRP1* genes to create auxotrophic strains. The resulting strains were tested for mating type and heterothallic status by using a pheromone assay described below or by crossing them with reference heterothallic haploid strains, allowing haploid heterothallic *MAT***a** or *MAT*α strains to be successfully isolated. Some double-transposase-inactivated strains did not mate with the reference strains, possibly because these are stable diploids or triploids (12) or possibly due to chromosomal rearrangements (43). Although we performed the gene inactivations individually, we later tested and verified that simultaneous targeting of both transposases with CRISPR$_{NHEJ}$ works efficiently in *K. marxianus*.

Mating pheromone response assay. We used reciprocal BLASTp using *S. cerevisiae* and *K. lactis* protein sequences as queries to identify two putative *MFA* genes (*KmMFA1* and *KmMFA2*), as well as the *MF*α gene (16, 17). The sequences in *S. cerevisiae* are encoded by genes YPL187W and YGL089C in the Saccharomyces Genome Database (44), and those in *K. lactis* are encoded by GenBank entry CAG99901.1 (RefSeq ID XP_454814.1) and as described in reference 17. To the best of our knowledge, these pheromones had not been previously identified in *K. marxianus*. We found two putative *MFA* genes (*KmMFA1* and *KmMFA2*) as well as the *MF*α gene (*KmMFα1*, which encodes 2 isotypes, *Km*MFα1 and *Km*MFα2) by reciprocal BLASTp using the *S. cerevisiae* and *K. lactis* protein sequences as queries (Table S2). Interestingly, the deduced **a**-factor amino acid sequences of *Km*MFa1 and *Km*MFa2 are not completely conserved, differing by 1 amino acid (Fig. 1C). Sequencing of *KmMFA1*, *KmMFA2*, and *KmMFα* from 8 unique strains shows full strain-to-strain conservation. Notably, *Km*MFa1 is completely conserved with the respective *K. lactis* sequence, suggesting a relatively conserved sexual cycle.

Synthetic **a**- and α-pheromones were obtained from Genemed Synthesis, Inc., and resuspended in water. To verify if the putative α-factors (*Km*MFα1 and *Km*MFα2) are viable and induce mating projections ("shmoo") in engineered heterothallic cells, we performed a pheromone morphological response assay. Cells were grown in YPD medium to a density of 10⁶ cells/100 ml, and both pheromones were added to a final concentration of 25 mg/ml. Cells were then examined under the light microscope at different times. Mating projections were observed after 6 h for the mature α-factors *Km*Mfα1 and *Km*Mfα2, while no morphological differences were seen in the absence of synthetic pheromone. Strains sensitive to the α-pheromones were classified as putative *MAT***a**, and strains that exhibited no mating projections in the presence of either α-pheromone for 12 h were presumed to be stable *MAT*α haploids or *MAT***a**/*MAT*α diploid strains. The mating type of heterothallic strains was verified by sequencing of the *MAT* loci, by PCR amplification of the *MAT* loci with primers flanking the *MAT* loci, and by *MAT*-specific primers (Table S2 and Fig. S2). The same procedure was done using the synthesized **a**-factors, but they failed to induce mating projections in the strains tested, possibly because **a**-factors are reported to be heavily posttranslationally modified, unlike α-factors (45).

K. marxianus auxotrophic mating. Auxotrophic double mutant strains (*α3⁻ kat1⁻*) of either mating type were grown up overnight from a single colony in 5 ml SCD medium. Strains were pelleted at 3,500 × *g* for 5 min, followed by washing with 1 ml of sterile water. Strains were pelleted again and resuspended in 50 μl of water. Four microliters of the cell suspension was dispensed as a single drop (patched) onto 2% glucose plates or MA5 plates and allowed to dry. Strains to be mated containing a complementary auxotrophic marker (either *leu2⁻* or *trp1⁻*) were dispensed on top of previous dried spots and allowed to mate at room temperature for 24 to 48 h. Mating plates were replica plated onto SCD agar plates minus both leucine and tryptophan. Diploid cells were grown at 30°C for 48 h. Freezer stocks were made by scraping off the diploid patch, resuspending in 25% glycerol, and freezing at −80°C.

Sporulation and spore purification. For sporulation, diploid strains were taken from freezer stocks and streaked onto an SCD agar plate minus leucine and tryptophan to ensure diploid strain growth. Single colonies were inoculated in 5 ml SCD liquid medium and grown overnight at 30°C. Many strains (including Km17) were observed to be unstable as diploids, and this treatment alone resulted in 25 to 90% sporulation. Strains or crosses that resulted in relatively stable diploids were then patched onto MA5 or SPO plates or suspended in 1 ml of M5 or SPO liquid medium and incubated at room temperature. Cells were observed under the optical microscope every 24 h for sporulation. Typically, sporulation was rapid and reached 25 to 95% sporulation in 24 h. However, recalcitrant strains would require up to 3 to 4 days.

Spore purification was performed as described previously (46). Diploid cultures from sporulation medium (MA5 or SPO medium) were scraped from solid medium or centrifuged at 3,500 $\times$ *g* from liquid medium for 5 min, resuspended into softening buffer (10 mM DTT, 100 mM Tris-SO$_4$ [pH 9.4]) at a cell/spore density of ~1 $\times$ 10^8/ml, and incubated for 10 min at 30°C. The spore/cell suspensions were centrifuged at 3,500 $\times$ *g* and suspended in spheroplasting buffer (2.1 M sorbitol, 10 mM potassium phosphate [pH 7.2]) to ~3 $\times$ 10^8 cell spores/ml. Zymolyase-100T (United States Biological Corporation; Fisher Scientific) was added to a final concentration of 0.2 mg/ml, and the mixture was incubated at 30°C for 20 min. Spheroplasts and spores were centrifuged at 3,500 $\times$ *g* for 5 min, and spheroplasts were lysed by multiple washes with 0.5% Triton X-100.

Complementation mating assay. To further validate the role of α3 and Kat1 in switching mating types, we constructed expression plasmids containing the coding sequences of each protein to perform a complementation assay. The proteins were cloned into the same vector used for Cas9 expression, under the control of the moderate-strength promoter of the gene *KmRNR2*. Alternative plasmids bearing the native promoter of *KAT1* or *ALPHA3* were also constructed. These plasmids were transformed into α3$^-$ *kat1$^-$ leu2$^-$* strains of either mating type. To test transformants for mating-type switching, we crossed them with stable heterothallic reference strains of either *MAT***a** or *MAT*α mating types that also lack the ability to produce tryptophan (α3$^-$ *kat1$^-$ trp1$^-$*). We inoculated 12 single transformants of each mating type in 20 ml of SCD medium and incubated them for 24 h at 30°C and 220-rpm shaking. The cultures were then washed and resuspended in 70 μl of water. Four microliters of each cell concentrate was spotted onto glucose 2% agar plates to induce switching and, later, mating. Reference strains of the same and opposite mating type were spotted on top of the 12 spots of transformants. The plates were incubated for 24 or 48 h at room temperature and then replica plated onto SCD − (Leu, Trp) plates. Growth was only observed in spots where mating occurred.

Culture conditions for inducing lipogenesis. Single colonies were grown overnight in 3 ml of YPD medium at 30°C and 225 rpm. Then 20 ml of YPD medium was inoculated with 0.5 ml of the overnight culture and grown at 30°C and 225 rpm for 24 h. Cells were pelleted at 3,000 $\times$ *g* for 10 min, washed with 1 ml of water, and then transferred to 1.5-ml tubes before being pelleted again at 3,000 $\times$ *g* for 10 min. The pellet was resuspended in 1 ml of lipogenesis medium and transferred to a 12-ml round-bottom tube containing 3 ml of the same medium. For the strains containing overexpression plasmids, the lipogenesis medium had 1 g/liter of monosodium glutamate instead of ammonium sulfate due to Geneticin's incompatibility with ammonium sulfate. Cultures were then shaken at 275 rpm at 42°C for 24 h. Cells were harvested by transferring 250 μl of each culture to preweighed Eppendorf tubes, spinning down at 3,000 $\times$ *g* for 10 min, washing with 500 μl of water, and then resuspending the culture in 100 μl of water prior to freezing it in liquid nitrogen. Cells were kept at −80°C prior to lyophilization. Culturing conditions for cellobiose-grown samples were similar, except that lipogenesis medium contained 8% cellobiose instead of glucose.

Epifluorescence microscopy and flow cytometry. To assay lipid production, *K. marxianus* cells were stained with the lipophilic dye Nile red (MP Biomedicals) which is permeable to yeast cells and a common indicator of intracellular lipid content. Single colonies of *K. marxianus* were grown in 3 ml of YPD medium overnight for at 30°C with 250-rpm shaking. Cell concentrations were then normalized, inoculated in fresh lipogenesis medium, and grown for 24 h at 42°C at 250 rpm. Cells were harvested by spinning down 1 OD$_{600}$ unit at 3,000 $\times$ *g* for 3 min and then resuspended in 500 μl of phosphate-buffered saline (PBS) solution (Sigma Aldrich). Then 6 μl of 1 mM Nile red solution (in dimethyl sulfoxide [DMSO]) was added to the cells, and the mixture was incubated in the dark at room temperature for 15 min. Cells were spun down and washed in 800 μl of ice-cold water, spun down again, and resuspended in another 800 μl ice-cold water. Nile red-stained cells were examined on a Zeiss Axioskop 2 epifluorescence microscope at 553-nm excitation and 636-nm emission.

For flow cytometry, 300 μl cell solution was diluted in 1 ml of ice-cold water and tested in the BD Biosciences Fortessa X20 fluorescence-activated cell sorter (FACS) using a 25,000-cell count, a forward scatter of 250, a side scatter of 250, and the 535LP and 585/42BP filters for fluorescence detection. Fluorescence data were analyzed using FlowJo software (Tree Star, Inc., Ashland, OR), and mean fluorescence values were obtained.

Isolation of high-lipid-producing strains. Strains Km19 and Km17 were made heterothallic by CRISPR$_{NHEJ}$ by inactivating both the *KAT1* and *ALPHA3* genes, as well as *TRP1* or *LEU2* (Table S1) to allow selection of diploids in SCD − (Leu, Trp) medium. Although Km19 does not transform well, by using our high-efficiency transformation protocol, we were able to recover a few colonies that transformed with the pKCas9 plasmid and allowed isolation of α3$^-$ *kat1$^-$* auxotrophic strains. Km17 had a much higher transformation success rate, and triple-inactivation strains were easily constructed. To select for thermotolerant and lipogenic strains, Km19 *MAT***a** α3$^-$ *kat1$^-$ trp1$^-$* was crossed with Km17 *MAT*α α3$^-$ *kat1$^-$ leu2$^-$* on MA5 medium (Table S1). Diploid cells were sporulated, and a spore suspension was made. Spores were germinated in YPD liquid medium overnight at 30°C, plated onto YPD plates, and incubated at 44°C to select for thermotolerant strains. Ninety-one colonies were then selected and subjected to

lipogenesis conditions for 24 h. The strains were ranked by Nile red mean fluorescence (Fig. S6), and those prone to flocculation as determined by light microscopy were eliminated from further analysis.

Determination of fatty acids by gravimetric analysis and GC-FID. To measure the percentage of fatty acids in dry cell weight, we extracted lipids from lyophilized cells and performed gravimetric analysis. Briefly, 250 μl of culture was pelleted at 4,000 $\times$ g for 10 min in preweighed 1.5-ml microcentrifuge tubes (Metter Toledo Excellence XS205DU balance). After the supernatant was removed, the cell pellet was suspended in 0.5 ml of water and pelleted again at 3,000 $\times$ g for 10 min, after which the pellet was resuspended in 100 μl of water. The samples were frozen and stored at −80°C. Frozen samples were then lyophilized overnight and weighed to calculate dry cell weight.

To measure the percentage of fatty acids in the different strains, we extracted lipids from lyophilized cells prepared as described above and analyzed them by gas chromatography. Fatty acids were extracted and transesterified into fatty acid methyl esters (FAMEs) with methanol in the presence of an acid catalyst. The dry cell pellet was transferred to 15-ml glass conical screw-top centrifuge tubes, and 1 ml of methanolic HCl (3 N concentration) with 2% chloroform was added to the pellet. To ensure complete transesterification, an additional 2 ml of methanolic HCl (3 N) plus 2% chloroform was added. Approximately 100 μg of an internal standard (methyl tridecanoate) with its exact mass recorded was prepared in methanol and was added to the tube. The tube was sealed with a Teflon-coated screw cap and heated at 85°C for 1.5 h with vortexing every 15 min. The mixture was then cooled to room temperature, and the resulting FAMEs were extracted by the addition of 1 ml of hexanes followed by 30 s of vortexing. An organic top layer was obtained by centrifugation of the sample at 3,000 $\times$ g for 10 min. The top layer was carefully collected and transferred to a GC vial. One microliter was injected in split mode (1:10) onto an SP2330 capillary column (30 m by 0.25 mm by 0.2 μm; Supelco). An Agilent 7890A gas chromatograph equipped with a flame ionization detector was used for analysis with the following instrumental settings: injector temperature, 250°C; carrier gas, helium at 1 ml/min; and temperature program, 140°C, 3 min isocratic, 10°C/min to 220°C, 40°C/min to 240°C, and 2.5 min isocratic.

Total oil extraction from dry yeast cells for thin-layer chromatography. Total yeast oil was extracted following the protocol described by Folch et al (47) for analysis by thin-layer chromatography. Approximately 20 mg dry cell weight and 500 mg silica beads were weighed into a 2-ml centrifuge tube. One milliliter MeOH was added to the tube, and it was vortexed. Then, the tube was put into an aluminum block and bead-beaten 4 times for 30 s with 30-s resting intervals in between. The contents were transferred into a conical 15-ml glass centrifuge tube, and 0.25 ml MeOH was used to rinse the residuals on the small centrifuge tube. CHCl$_3$ (2.5 ml) was added, and the tube was briefly vortexed. The tube was shaken for 1 h at 235 rpm. Two hundred fifty microliters of CHCl$_3$-MeOH (2:1) and 1 ml of MgCl$_2$ (aqueous) (0.034%) were added into the mixture, and the tube was shaken for 10 min. The solution was vortexed for 30 s and centrifuged at 3,000 rpm for 5 min, and the upper aqueous layer was removed. The resulting organic layer was washed with 1 ml 2 N KCl-methanol (4:1 vol/vol), vortexed, and centrifuged in the same way. The aqueous upper layer was removed, and the resulting organic layer was introduced with the artificial upper phase (chloroform-methanol-water at 3:48:47). The resulting mixture was vortexed and centrifuged, and the upper layer was aspirated. This step involving the artificial upper phase was repeated until the white layer at the interface completely disappeared.

Thin-layer chromatography analysis of lipid composition. TLC plates (7 by 10 cm) were preheated in a 120˚C oven for at least 10 min. A piece of paper towel/filter paper (7 by 10 cm) was added into a 600-ml beaker for saturation, and solvent system 1 (SS1: petroleum ether-Et$_2$O-AcOH [70:30:2]) was added until the solvent reached about 0.5 to 1 cm in height. The beaker was covered with aluminum foil and Parafilm, and the resulting setup was left alone for at least 10 min. Compounds were spotted on the preheated TLC plate, and the plate ran in SS1 until the solvent front was halfway up the plate. The plate was dried at room temperature for 15 min. The plate was run using solvent system 2 (SS2: petroleum ether-Et$_2$O [98:2]) until the solvent front nearly reached the top of the plate. The resulting TLC plate was dried under a fume hood for 30 min before being immersed in MnCl$_2$ charring solution (0.63 g MnCl$_2$·4H$_2$O, 60 ml H$_2$O, 60 ml MeOH, 4 ml concentrated H$_2$SO$_4$) for 10 s. The stained plate was developed in a 120˚C oven for approximately 20 min or until dark spots were observed.

Data availability. The raw fastq reads have been deposited in the NCBI SRA (accession no. SRP158013) and the scaffolds and annotation in Genbank under BioSample accession no. SAMN09839046.

SUPPLEMENTAL MATERIAL

Supplemental material for this article may be found at https://doi.org/10.1128/mBio .01410-18.

FIG S1, TIF file, 2.6 MB.
FIG S2, TIF file, 0.6 MB.
FIG S3, TIF file, 1.7 MB.
FIG S4, TIF file, 0.3 MB.
FIG S5, TIF file, 0.9 MB.
FIG S6, TIF file, 0.3 MB.
FIG S7, TIF file, 0.8 MB.
TABLE S1, XLSX file, 0.1 MB.
TABLE S2, XLSX file, 0.1 MB.

REFERENCES

1. Löbs A-K, Schwartz C, Wheeldon I. 2017. Genome and metabolic engineering in non-conventional yeasts: current advances and applications. Synth Syst Biotechnol 2:198–207. https://doi.org/10.1016/j.synbio.2017.08.002.

2. Groeneveld P, Stouthamer AH, Westerhoff HV. 2009. Super life—how and why "cell selection" leads to the fastest-growing eukaryote. FEBS J 276:254–270. https://doi.org/10.1111/j.1742-4658.2008.06778.x.

3. Banat IM, Nigam P, Marchant R. 1992. Isolation of thermotolerant, fermentative yeasts growing at 52°C and producing ethanol at 45°C and 50°C. World J Microbiol Biotechnol 8:259–263. https://doi.org/10.1007/BF01201874.

4. Yarimizu T, Nonklang S, Nakamura J, Tokuda S, Nakagawa T, Lorreungsil S, Sutthikhumpha S, Pukahuta C, Kitagawa T, Nakamura M, Cha-Aim K, Limtong S, Hoshida H, Akada R. 2013. Identification of auxotrophic mutants of the yeast Kluyveromyces marxianus by non-homologous end joining-mediated integrative transformation with genes from Saccharomyces cerevisiae. Yeast 30:485–500. https://doi.org/10.1002/yea.2985.

5. Lane MM, Burke N, Karreman R, Wolfe KH, O'Byrne CP, Morrissey JP. 2011. Physiological and metabolic diversity in the yeast Kluyveromyces marxianus. Antonie Van Leeuwenhoek 100:507–519. https://doi.org/10.1007/s10482-011-9606-x.

6. Nambu-Nishida Y, Nishida K, Hasunuma T, Kondo A. 2017. Development of a comprehensive set of tools for genome engineering in a cold- and thermo-tolerant Kluyveromyces marxianus yeast strain. Sci Rep 7:8993. https://doi.org/10.1038/s41598-017-08356-5.

7. Löbs A-K, Engel R, Schwartz C, Flores A, Wheeldon I. 2017. CRISPR-Cas9-enabled genetic disruptions for understanding ethanol and ethyl acetate biosynthesis in Kluyveromyces marxianus. Biotechnol Biofuels 10:164. https://doi.org/10.1186/s13068-017-0854-5.

8. Lee M-H, Lin J-J, Lin Y-J, Chang J-J, Ke H-M, Fan W-L, Wang T-Y, Li W-H. 2018. Genome-wide prediction of CRISPR/Cas9 targets in Kluyveromyces marxianus and its application to obtain a stable haploid strain. Sci Rep 8:7305. https://doi.org/10.1038/s41598-018-25366-z.

9. Juergens H, Varela JA, Gorter de Vries AR, Perli T, Gast VJM, Gyurchev NY, Rajkumar AS, Mans R, Pronk JT, Morrissey JP, Daran J-MG. 2018. Genome editing in Kluyveromyces and Ogataea yeasts using a broad-host-range Cas9/gRNA co-expression plasmid. FEMS Yeast Res 18:foy012. https://doi.org/10.1093/femsyr/foy012.

10. Goddard MR, Godfray HCJ, Burt A. 2005. Sex increases the efficacy of natural selection in experimental yeast populations. Nature 434:636–640. https://doi.org/10.1038/nature03405.

11. van Zyl WH, Lodolo EJ, Gericke M. 1993. Conversion of homothallic yeast to heterothallism through HO gene disruption. Curr Genet 23:290–294. https://doi.org/10.1007/BF00310889.

12. Ortiz-Merino RA, Varela JA, Coughlan AY, Hoshida H, da Silveira WB, Wilde C, Kuijpers NGA, Geertman J-M, Wolfe KH, Morrissey JP. 2018. Ploidy variation in Kluyveromyces marxianus separates dairy and non-dairy isolates. Front Genet 9:94. https://doi.org/10.3389/fgene.2018.00094.

13. Ryan OW, Skerker JM, Maurer MJ, Li X, Tsai JC, Poddar S, Lee ME, DeLoache W, Dueber JE, Arkin AP, Cate JHD. 2014. Selection of chromosomal DNA libraries using a multiplex CRISPR system. elife 3:e03703. https://doi.org/10.7554/eLife.03703.

14. Barsoum E, Martinez P, Aström SU. 2010. Alpha3, a transposable element that promotes host sexual reproduction. Genes Dev 24:33–44. https://doi.org/10.1101/gad.557310.

15. Rajaei N, Chiruvella KK, Lin F, Aström SU. 2014. Domesticated transposase Kat1 and its fossil imprints induce sexual differentiation in yeast. Proc Natl Acad Sci U S A 111:15491–15496. https://doi.org/10.1073/pnas.1406027111.

16. Altschul SF, Gish W, Miller W, Myers EW, Lipman DJ. 1990. Basic local alignment search tool. J Mol Biol 215:403–410. https://doi.org/10.1016/S0022-2836(05)80360-2.

17. Ongay-Larios L, Navarro-Olmos R, Kawasaki L, Velázquez-Zavala N, Sánchez-Paredes E, Torres-Quiroz F, Coello G, Coria R. 2007. Kluyveromyces lactis sexual pheromones. Gene structures and cellular responses to alpha-factor. FEMS Yeast Res 7:740–747. https://doi.org/10.1111/j.1567-1364.2007.00249.x.

18. Fonseca GG, Heinzle E, Wittmann C, Gombert AK. 2008. The yeast Kluyveromyces marxianus and its biotechnological potential. Appl Microbiol Biotechnol 79:339–354. https://doi.org/10.1007/s00253-008-1458-6.

19. Pfeiffer T, Morley A. 2014. An evolutionary perspective on the Crabtree effect. Front Mol Biosci 1:17. https://doi.org/10.3389/fmolb.2014.00017.

20. Shi S, Ji H, Siewers V, Nielsen J. 2016. Improved production of fatty acids by Saccharomyces cerevisiae through screening a cDNA library from the oleaginous yeast Yarrowia lipolytica. FEMS Yeast Res 16:fov108. https://doi.org/10.1093/femsyr/fov108.

21. Greenspan P, Mayer EP, Fowler SD. 1985. Nile red: a selective fluorescent stain for intracellular lipid droplets. J Cell Physiol 100:965–973.

22. Athenstaedt K, Jolivet P, Boulard C, Zivy M, Negroni L, Nicaud J-M, Chardot T. 2006. Lipid particle composition of the yeast Yarrowia lipolytica depends on the carbon source. Proteomics 6:1450–1459. https://doi.org/10.1002/pmic.200500339.

23. Blazeck J, Hill A, Liu L, Knight R, Miller J, Pan A, Otoupal P, Alper HS. 2014. Harnessing Yarrowia lipolytica lipogenesis to create a platform for lipid and biofuel production. Nat Commun 5:3131. https://doi.org/10.1038/ncomms4131.

24. Boulton CA, Ratledge C. 1981. Correlation of lipid accumulation in yeasts with possession of ATP:citrate lyase. Microbiology 127:169–176. https://doi.org/10.1099/00221287-127-1-169.

25. Lazar Z, Dulermo T, Neuvéglise C, Crutz-Le Coq A-M, Nicaud J-M. 2014. Hexokinase—a limiting factor in lipid production from fructose in Yarrowia lipolytica. Metab Eng 26:89–99. https://doi.org/10.1016/j.ymben.2014.09.008.

26. Ida Y, Furusawa C, Hirasawa T, Shimizu H. 2012. Stable disruption of ethanol production by deletion of the genes encoding alcohol dehydrogenase isozymes in Saccharomyces cerevisiae. J Biosci Bioeng 113:192–195. https://doi.org/10.1016/j.jbiosc.2011.09.019.

27. Lin J-L, Zhu J, Wheeldon I. 2016. Rapid ester biosynthesis screening reveals a high activity alcohol-O-acyltransferase (AATase) from tomato fruit. Biotechnol J 11:700–707. https://doi.org/10.1002/biot.201500406.

28. Lanza AM, Alper HS. 2011. Global strain engineering by mutant transcription factors. Methods Mol Biol 765:253–274. https://doi.org/10.1007/978-1-61779-197-0_15.

29. Bassalo MC, Liu R, Gill RT. 2016. Directed evolution and synthetic biology applications to microbial systems. Curr Opin Biotechnol 39:126–133. https://doi.org/10.1016/j.copbio.2016.03.016.

30. Lam FH, Hartner FS, Fink GR, Stephanopoulos G. 2010. Enhancing stress resistance and production phenotypes through transcriptome engineering. Methods Enzymol 470:509–532. https://doi.org/10.1016/S0076-6879(10)70020-3.

31. Snoek T, Picca Nicolino M, Van den Bremt S, Mertens S, Saels V, Verplaetse A, Steensels J, Verstrepen KJ. 2015. Large-scale robot-assisted genome shuffling yields industrial Saccharomyces cerevisiae yeasts with increased ethanol tolerance. Biotechnol Biofuels 8:32. https://doi.org/10.1186/s13068-015-0216-0.

32. Meiron H, Nahon E, Raveh D. 1995. Identification of the heterothallic mutation in HO-endonuclease of S. cerevisiae using HO/ho chimeric genes. Curr Genet 28:367–373. https://doi.org/10.1007/BF00326435.

33. Klar AJ, Strathern JN, Abraham JA. 1984. Involvement of double-strand chromosomal breaks for mating-type switching in Saccharomyces

cerevisiae. Cold Spring Harbor Symp Quant Biol 49:77–88. https://doi.org/10.1101/SQB.1984.049.01.011.

34. Coïc E, Richard G-F, Haber JE. 2006. Saccharomyces cerevisiae donor preference during mating-type switching is dependent on chromosome architecture and organization. Genetics 173:1197–1206. https://doi.org/10.1534/genetics.106.055392.

35. Mlícková K, Roux E, Athenstaedt K, d'Andrea S, Daum G, Chardot T, Nicaud J-M. 2004. Lipid accumulation, lipid body formation, and acyl coenzyme A oxidases of the yeast Yarrowia lipolytica. Appl Environ Microbiol 70: 3918–3924. https://doi.org/10.1128/AEM.70.7.3918-3924.2004.

36. Zhou YJ, Buijs NA, Zhu Z, Qin J, Siewers V, Nielsen J. 2016. Production of fatty acid-derived oleochemicals and biofuels by synthetic yeast cell factories. Nat Commun 7:11709. https://doi.org/10.1038/ncomms11709.

37. Kang M-K, Nielsen J. 2017. Biobased production of alkanes and alkenes through metabolic engineering of microorganisms. J Ind Microbiol Biotechnol 44:613–622. https://doi.org/10.1007/s10295-016-1814-y.

38. Solovyev V, Kosarev P, Seledsov I, Vorobyev D. 2006. Automatic annotation of eukaryotic genes, pseudogenes and promoters. Genome Biol 7:S10.1–S12. https://doi.org/10.1186/gb-2006-7-s1-s10.

39. Salamov AA, Solovyev VV. 2000. Ab initio gene finding in Drosophila genomic DNA. Genome Res 10:516–522. https://doi.org/10.1101/gr.10.4.516.

40. Ogden RC, Adams DA. 1987. Electrophoresis in agarose and acrylamide gels. Methods Enzymol 152:61–87. https://doi.org/10.1016/0076-6879(87)52011-0.

41. Gietz RD. 2014. Yeast transformation by the LiAc/SS carrier DNA/PEG method, p 1–12. In Smith JS, Burke DJ (ed), Yeast genetics: methods and protocols. Springer, New York, NY.

42. Green MR, Sambrook J. 2016. Precipitation of DNA with ethanol. Cold Spring Harb Protoc 2016. https://doi.org/10.1101/pdb.prot093377.

43. Greig D. 2009. Reproductive isolation in Saccharomyces. Heredity 102: 39–44. https://doi.org/10.1038/hdy.2008.73.

44. Cherry JM, Hong EL, Amundsen C, Balakrishnan R, Binkley G, Chan ET, Christie KR, Costanzo MC, Dwight SS, Engel SR, Fisk DG, Hirschman JE, Hitz BC, Karra K, Krieger CJ, Miyasato SR, Nash RS, Park J, Skrzypek MS, Simison M, Weng S, Wong ED. 2012. Saccharomyces genome database: the genomics resource of budding yeast. Nucleic Acids Res 40: D700–D705. https://doi.org/10.1093/nar/gkr1029.

45. Michaelis S, Barrowman J. 2012. Biogenesis of the Saccharomyces cerevisiae pheromone a-factor, from yeast mating to human disease. Microbiol Mol Biol Rev 76:626–651. https://doi.org/10.1128/MMBR.00010-12.

46. Herman PK, Rine J. 1997. Yeast spore germination: a requirement for ras protein activity during re-entry into the cell cycle. EMBO J 16:6171–6181. https://doi.org/10.1093/emboj/16.20.6171.

47. Folch J, Lees M, Sloane Stanley GH. 1957. A simple method for the isolation and purification of total lipids from animal tissues. J Biol Chem 226:497–509.